

via 5- and 6-membered chelate rings [5]. The common oxidation states of copper are I (d^{10}), II (d^9), and III (d^8). The most common oxidation state of Cu is (II), and Cu(II) complexes have been extensively studied. These complexes have tetrahedral, octahedral, square planar and trigonal bipyramidal geometries [6]. Due to the presence of unpaired electron, all the copper(II) complexes are paramagnetic.

This chapter deals with the synthesis and characterization of mononuclear and binuclear Cu(II) complexes with different N(4)-ring incorporated thiosemicarbazone ligands. The structure of one of the compounds has been solved by single crystal X-ray diffraction studies and was found to be distorted square pyramidal in geometry.

3.2. Experimental

3.2.1. Materials

The thiosemicarbazone ligands were synthesized as discussed in Chapter 2 and solvents were purified by distillation. Pyridine, γ -picoline, 1,10-phenanthroline (Ranbaxy fine chemicals), 2,2'-bipyridine (Central drug house chemicals) and $\text{Cu}(\text{OAc})_2 \cdot \text{H}_2\text{O}$ (Fluka) were used as received.

3.2.2. Synthesis of the complexes

[CuL¹]₂·H₂O (1): This complex was synthesized by refluxing an ethanolic solution of HL¹ (2 mmol, 0.522 g) with an aqueous solution of $\text{Cu}(\text{OAc})_2 \cdot \text{H}_2\text{O}$ (1 mmol, 0.199 g) for 4 h. The complex formed was filtered, washed with ethanol and finally with ether and dried over P_4O_{10} *in vacuo*.

[[CuL²]₂] (2): This complex was synthesized by refluxing an ethanolic solution of H₂L² (1 mmol, 0.277 g) with an aqueous solution of $\text{Cu}(\text{OAc})_2 \cdot \text{H}_2\text{O}$ (1 mmol, 0.199 g) for 4 h in an alkaline medium. The brown colored product formed was filtered, washed with ethanol and finally with ether and dried over P_4O_{10} *in vacuo*.

[Cu(HL²)₂] (3): Ethanolic solution of the ligand H₂L² (2 mmol, 0.554 g) and an aqueous solution of Cu(OAc)₂·H₂O (1 mmol, 0.199 g) in 2:1 ratio was refluxed for 2-3 h. The complex formed was filtered, washed with ethanol and finally with ether and dried over P₄O₁₀ *in vacuo*.

[CuL²bipy] (4): To a solution of H₂L² (1 mmol, 0.277 g) in hot ethanol was added heterocyclic base 2,2'-bipyridine (1 mmol, 0.156 g) with constant stirring. To this was added an aqueous solution of Cu(OAc)₂·H₂O (1 mmol, 0.199 g) and the resulting solution was then refluxed for 3 h. The product formed was filtered, washed with ethanol and finally with ether and dried over P₄O₁₀ *in vacuo*.

[CuL²phen] (5): Solutions of H₂L² (1 mmol, 0.277 g) and heterocyclic base 1,10-phenanthroline (1 mmol, 0.198 g) were mixed and to this was added an aqueous solution of Cu(OAc)₂·H₂O (1 mmol, 0.199 g) and refluxed for 2-3 h. The green colored product formed was filtered, washed with ethanol and finally with ether and dried over P₄O₁₀ *in vacuo*.

[CuL²γ-pic]·2H₂O (6): The H₂L² (1 mmol, 0.277 g) was dissolved in ethanol, to which was added a slight excess of heterocyclic base γ-picoline (3 mmol, 0.279 g) with constant stirring. This was followed by the addition of an aqueous solution of Cu(OAc)₂·H₂O (1 mmol, 0.199 g) and then refluxed for 4h. The resulting solution was then concentrated on a water bath and cooled at room temperature, filtered and kept overnight. The brown colored product formed was filtered, washed with ethanol and ether and dried *in vacuo* over P₄O₁₀.

[CuL³]₂·0.5H₂O (7): Ethanolic solutions of the ligand HL³ (2 mmol, 0.582 g) and Cu(OAc)₂·H₂O (1 mmol, 0.199 g) in 2:1 ratio was refluxed for 2 h. The complex formed was filtered, washed with ethanol and finally with ether and dried over P₄O₁₀ *in vacuo*.

[Cu(HL⁴)₂] (8): This complex was synthesized by refluxing an ethanolic solution

of H_2L^4 (2 mmol, 0.498 g) with an aqueous solution of $\text{Cu}(\text{OAc})_2 \cdot \text{H}_2\text{O}$ (1 mmol, 0.199 g) for 4 h. The complex formed was filtered, washed with ethanol and finally with ether and dried over P_4O_{10} *in vacuo*.

[CuL⁴py]·3H₂O (9): To a hot ethanolic solution of the ligand H_2L^4 (1 mmol, 0.249 g), added an aqueous solution of $\text{Cu}(\text{OAc})_2 \cdot \text{H}_2\text{O}$ (1 mmol, 0.199 g) with constant stirring. This was followed by the addition of slight excess of the base pyridine (3 mmol, 0.237 g). The above brown solution was then refluxed for about 3 h. The complex formed was filtered, washed with ethanol and ether and dried *in vacuo* over P_4O_{10} .

[CuL⁴bipy] (10): An ethanolic solution of H_2L^4 (1 mmol, 0.249 g) was mixed with an aqueous solution of $\text{Cu}(\text{OAc})_2 \cdot \text{H}_2\text{O}$ (1 mmol, 0.199 g) and this was followed by the addition of the base bipy (1 mmol, 0.156 g) in the solid form. The resulting solution was then refluxed for 2h, when green shining crystals began to separate. This was filtered, washed with ethanol and ether and dried *in vacuo* over P_4O_{10} .

3.2.3. Physical measurements

Elemental analyses were carried out using a Vario EL III CHN analyzer at SAIF, Kochi, India. Magnetic susceptibility measurements were carried out at IIT, Roorkee, at room temperature in the polycrystalline state on a PAR model 155 Vibrating Sample Magnetometer (VSM) at 5 k Oe. field strength using $\text{Hg}[\text{Co}(\text{SCN})_4]$ as a calibrant. Diamagnetic corrections were made using Pascal's constants. The FT-IR spectra were recorded on a Thermo Nicolet AVATAR 370 DTGS FTIR Spectrometer using KBr pellets in the range 500-4000 cm^{-1} at SAIF, Cochin University of Science and Technology, Kochi 22, India and Far-IR spectra were recorded in the range 50-500 cm^{-1} on a Nicolet Magna 550 FT-IR spectrophotometer using polyethylene pellets at SAIF, IIT, Bombay, India. Electronic spectra were recorded on a UVD-3500 UV-VIS-Double beam

Spectrophotometer from solutions in DMF. The EPR spectra were recorded on a Varian E-112 Spectrometer using TCNE as the standard at SAIF, IIT, Bombay, India.

3.2.4. X-ray crystallography

A dark green crystal of the compound **10** having approximate dimensions $0.35 \times 0.20 \times 0.15 \text{ mm}^3$ was sealed in a glass capillary and intensity data were measured at room temperature (293 K). The crystallographic data and structure refinement parameters for the compound are given in Table 3.1.

Table 3.1. Crystal data and experimental parameters for compound **10**

Empirical formula	$\text{C}_{22} \text{H}_{21} \text{Cu N}_5 \text{O S}$
Temperature	293(2) K
Formula weight	467.06
Wavelength	0.71073 Å
Crystal system	Monoclinic
Space group	$P 2_1/n$
Unit cell dimensions	$a = 9.0400(5) \text{ Å}$ $b = 19.773(2) \text{ Å}$ $c = 12.613(3) \text{ Å}$ $\alpha = 90^\circ$ $\beta = 108.590(12)^\circ$ $\gamma = 90^\circ$
Volume	$2136.9(6) \text{ Å}^3$
Z	4
Calculated density	1.452 g/cm^3
Absorption coefficient	1.143 mm^{-1}
F(000)	964
Crystal size	$0.35 \times 0.20 \times 0.15 \text{ mm}^3$
θ range for data collection	1.99 to 24.99°
Index ranges	$-10 \leq h \leq 10, -23 \leq k \leq 0, -14 \leq l \leq 0$
Reflections collected	3914
Independent reflections	3736 [R(int) = 0.0298]
Refinement method	Full-matrix least-squares on F^2
Data / restraints / parameters	3736 / 0 / 271
Goodness-of-fit on F^2	1.024
Final R indices [$I > 2\sigma(I)$]	$R1 = 0.0428, wR2 = 0.0914$
R indices (all data)	$R1 = 0.1028, wR2 = 0.1058$

The X-ray diffraction data were measured at room temperature and data acquisition and cell refinement were done using the Argus (Nonius, MACH3 software) [7]. The Maxus (Nonius software) were used for data reduction [8]. The structure was solved by direct methods with the program SHELXS-97 and refined by full matrix least squares on F^2 using SHELXL-97 [9]. The graphical tool used was DIAMOND version 3.1d [10]. All non-hydrogen atoms were refined anisotropically and all hydrogen atoms were geometrically fixed at calculated positions.

3.3. Results and discussion

The ligands gave complexes more readily under reflux in the aqueous-ethanol/methanol medium. Complexes **1**, **6**, **7** and **9** contain uncoordinated water molecules. The complexes **1**, **3**, **7** and **8** were readily formed by refluxing their respective ligands and $\text{Cu}(\text{OAc})_2 \cdot \text{H}_2\text{O}$ in 2:1 ratio and have the general formula $[\text{ML}_2]$ (for complexes **1** and **7**) and $[\text{M}(\text{HL})_2]$ (for complexes **3**, and **8**). The complex **2** was prepared using H_2L^2 ligand and $\text{Cu}(\text{OAc})_2 \cdot \text{H}_2\text{O}$ in 1:1 ratio in alkaline medium and has the general formula $[(\text{ML})_2]$. The complexes **4**, **5**, **6**, **9** and **10** were assigned the general formula MLB , where B are heterocyclic bases, pyridine, 2,2'-bipyridine, 1,10-phenanthroline or γ -picoline and were prepared by refluxing their respective ligands with $\text{Cu}(\text{OAc})_2 \cdot \text{H}_2\text{O}$ and heterocyclic bases in the 1:1:1 ratio. From the structural, elemental and spectral studies, the compounds **1-10** were assigned the empirical formula $[\text{CuL}^1_2]$ (**1**), $[(\text{CuL}^2)_2]$ (**2**), $[\text{Cu}(\text{HL}^2)_2]$ (**3**), $[\text{CuL}^2\text{bipy}]$ (**4**), $[\text{CuL}^2\text{phen}]$ (**5**), $[\text{CuL}^2\gamma\text{-pic}] \cdot 2\text{H}_2\text{O}$ (**6**), $[\text{CuL}^3_2] \cdot 0.5\text{H}_2\text{O}$ (**7**), $[\text{Cu}(\text{HL}^4)_2]$ (**8**), $[\text{CuL}^4\text{py}] \cdot 3\text{H}_2\text{O}$ (**9**), $[\text{CuL}^4\text{bipy}]$ (**10**) respectively and X-ray quality single crystals of the complex **10** were obtained from its solution in methanol by slow evaporation over a period of 8 days. The analytical data of the complexes are presented in Table 3.2.

Table 3.2. Analytical data

Compound	color	μ_{eff} (B.M)	Anal: Found (Calcd.) %		
			C	H	N
[CuL ¹] ₂ ·H ₂ O (1)	brown	2.02	56.00(55.83)	6.20(6.36)	13.97(13.95)
[(CuL ²) ₂] (2)	brown	1.25	50.08(49.60)	4.73(5.06)	12.25(12.40)
[Cu(HL ²) ₂] (3)	brown	2.04	54.35(54.57)	6.12(5.89)	13.63(13.64)
[CuL ³ bipy] (4)	green	1.64	57.99(58.22)	5.12(5.09)	14.10(14.15)
[CuL ³ phen] (5)	green	1.59	60.05(60.16)	4.90(4.85)	13.43(13.49)
[CuL ³ γ -pic]·2H ₂ O (6)	brown	1.54	51.74(51.32)	5.60(6.03)	12.34(11.97)
[CuL ³] ₂ ·0.5H ₂ O (7)	brown	1.62	55.38(55.15)	6.82(6.33)	12.91(12.86)
[Cu(HL ⁴) ₂] (8)	brown	1.92	51.44(51.46)	4.91(5.04)	14.89(15.00)
[CuL ⁴ py]·3H ₂ O (9)	brown	1.65	45.36(45.99)	4.62(5.15)	13.10(12.62)
[CuL ⁴ bipy] (10)	green	1.52	56.42(56.58)	4.45(4.53)	14.88(14.99)

Magnetic moments of the complexes were calculated from magnetic susceptibility measurements. Mononuclear Cu(II) complexes exhibit magnetic moments in the range 1.5-2.05 B.M, which are close to their spin-only value. Magnetic moment of binuclear Cu(II) complex **2** is 1.25 B.M which was in the range of 1.15-1.40 B.M, found for binuclear complexes. This low magnetic moment may be attributed to the presence of a strong antiferromagnetic spin-spin interaction involving an oxygen-bridged binuclear structure similar to those proposed for the Cu(II) complexes of analogous tridentate ligands [11].

3.3.1. Crystal structure of [CuL⁴bipy]

The molecular structure of the compound along with atom numbering scheme is given in Figure 3.1 and selected bond lengths and bond angles are summarized in Table 3.3.

The compound crystallized with one monomer per asymmetric unit into monoclinic crystal system with a space group *P21/n*. The copper in the

mononuclear complex is five coordinated and is having an approximate square pyramid (SPY) geometry around the copper(II) ion. The copper centre is coordinated by the phenolato oxygen, O1, azomethine nitrogen N1, and the thiolato sulphur S1, of the thiosemicarbazone and the pyridine nitrogens N5 and N4, of bipyridine. The donor atoms O1, N1, S1 of the thiosemicarbazone and N5 of the bipyridine occupy the equatorial position and the other bipyridine nitrogen N4 occupies the axial position at a larger distance. The large bond distance at the axial Cu1–N4 position supports the lack of out of plane π -bonding. This fact is in accordance with the absence of superhyperfine splitting due to N4 in the EPR spectrum of the compound. The Cu–N and Cu–O bond lengths vary in the range 1.951(4) to 2.016(4) Å. The C7–N1 and N2–C8 bond lengths are comparable to that for C=N bond length. Of these two, N2–C8 bond length is larger due to enolization of the ligand in complex formation. The O1–Cu1–N4 and S1–Cu1–N4 bond angles indicate a slight tilting of the axial Cu1–N4 bond in the direction of O1–Cu1 bond and away from the S1–Cu1 bond. The N4–Cu1–S1 bond angle is shorter compared to our previous reports [12, 13]. The Cu1–N1 bond length is shorter compared to the Cu–N bond lengths of bipyridine indicates that the thiosemicarbazone moiety dominates equatorial bonding. The rather small bite angle [N1–Cu1–S1= 85.27(9)° and O1–Cu1–S1= 164.44(9)°] defines largest distortion of the geometry. One of the reasons for the deviation from an ideal stereochemistry is the restricted bite angle imposed by both the L²⁻ and bipy ligands. The bite angle around the metal *via* N4–Cu1–N5 of 76.95(12)° may be considered normal, when compared with an average value of 77° cited in the literature [12, 14-16]. In a five-coordinated system, the angular structural parameter (τ) is used to propose an index of trigonality. The τ is defined by $\tau = (\alpha - \beta) / 60$, (Where $\tau = 0$ for a square pyramidal geometry and 1 for trigonal bipyramidal geometry), and α and β are the trans angles [17]. The τ value for the complex is

0.15, indicates that the coordination around Cu(II) is best described as distorted square pyramid with copper displaced by 0.1921(5) Å from the plane containing the four donor atoms N5, S1, N1 and O1 towards the pyridyl nitrogen N4, which is evident from the bond angles of N1–Cu1–N5= 173.28(13)°, and O1–Cu1–S1= 164.44(9)°.

Table 3.3. Selected bond lengths (Å) and bond angles (°) for [CuL⁴bipy]

Bond lengths (Å)		Bond angles (°)	
Cu1–O1	1.954(3)	O1–Cu1–N1	92.89(12)
Cu1–N1	1.952(3)	O1–Cu1–N5	89.66(11)
Cu1–N5	2.050(3)	N1–Cu1–N5	173.28(13)
Cu1–N4	2.227(3)	O1–Cu1–N4	95.43(11)
Cu1–S1	2.273(11)	N1–Cu1–N4	108.96(12)
S1–C8	1.743(4)	N4–Cu1–N5	76.95(12)
O1–C1	1.314(5)	O1–Cu1–S1	164.44(9)
N1–C7	1.296(5)	N1–Cu1–S1	85.27(9)
N1–N2	1.396(4)	N5–Cu1–S1	90.60(9)
N2–C8	1.317(5)	N4–Cu1–S1	99.79(8)
N3–C8	1.348(5)		

The dihedral angle formed by the least square plane Cg(1) and Cg(4) is 11.12° [Cg(1)= Cu1, N1, N2, C8, S1 and Cg(4)= Cu1, O1, C1, C6, C7, N1]. This small deviation from coplanarity would certainly not hinder the delocalization of electrons in the coordination sphere, and the stability of the complex is sustained.

Ring puckering analysis indicates that Cg(3) ring comprising of N3, C9, C10, C11 and C12 adopts an envelop conformation on C11. [$\theta(2)$ = 0.1955 Å and $\phi(2)$ = 103.5615°]

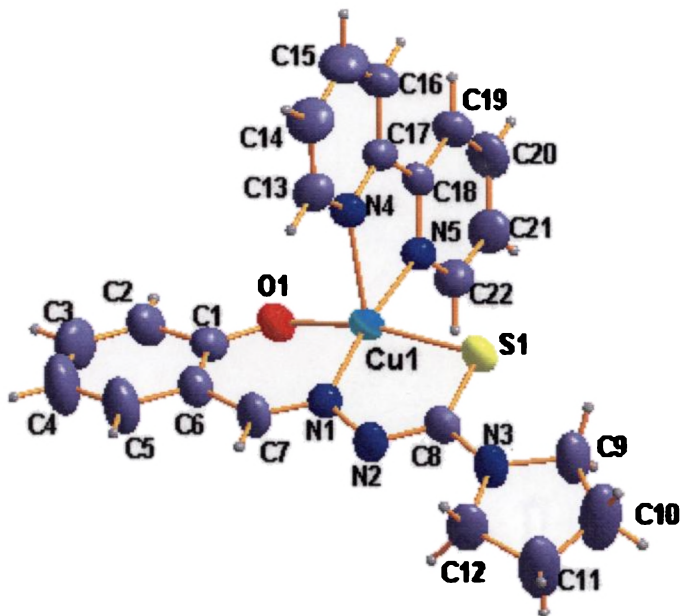


Figure 3.1. Structure and labeling scheme for $[\text{CuL}^4\text{bipy}]$ (10)

The unit cell is viewed along the c axis and four molecules are arranged in the unit volume cell (Figure 3.2). The packing of the molecules is stabilized by intermolecular hydrogen bonding, π - π and $\text{CH}\dots\pi$ interactions. These interactions are given in Table 3.4. The centroid $\text{Cg}(5)$ is involved in π - π interactions with pyridyl ring of the neighbouring unit at a distance of 3.5912 Å. The intermolecular hydrogen bonding involving atoms H13 and H14 with N2, H15 with S1 and H16, H19, H21 and H22 with O1 respectively, reinforce crystal structure cohesion in the close packing. In addition to the intermolecular hydrogen bonding, the $\text{CH}\dots\pi$ interactions of the pyridyl hydrogen of the bipyridine with the metal chelate rings of the neighbouring molecules contributes to the stability of the unit cell packing.

Table 3.4. Interaction parameters of the compound 10

 π - π interactions

Cg(I)-Res(1)⋯Cg(J)	Cg-Cg (Å)	α°	β°
Cg(5) [1] -> Cg(6) ^a	3.5912	3.72	21.17
Cg(6) [1] -> Cg(5) ^a	3.5912	3.72	23.11

Equivalent position code: a= -x, -y, -z

Cg(5)= N4, C13, C14, C15, C16, C17; Cg(6)= N5, C18, C19, C20, C21, C22

CH- π interactions

X-H(I)⋯Cg(J)	H...Cg (Å)	X-H...Cg (°)	X...Cg (Å)
C15-H15 [1] -> Cg(1) ^a	2.73	146	3.5377

Equivalent position code: a= -1+x, y, z

Cg(1)= Cu1, N1, N2, C8, S1

H-bonding

D-H...A	D...H (Å)	H...A (Å)	D...A (Å)	D-H...A (°)
C13-H13...N2 ^a	0.930	2.649(1)	3.555(1)	164.88(1)
C14-H14...N2 ^b	0.930	2.927	3.616	132(2)
C15-H15...S1 ^b	0.930	2.785	3.699	167.70(1)
C16-H16...O1 ^c	0.930	2.855(1)	3.690(1)	150.12(2)
C19-H19...O1 ^c	0.930	2.739	3.587	152.07(2)
C21-H21...O1 ^d	0.930	2.876	3.443	120.60(2)
C22-H22...O1 ^d	0.930	2.671	3.360	131.50(2)

D=donor, A=acceptor, Equivalent position code: a= -x+1, -y, -z+1; b= x-1, +y,+z; c= -x,-y,-z; d= -x+1,-y,-z

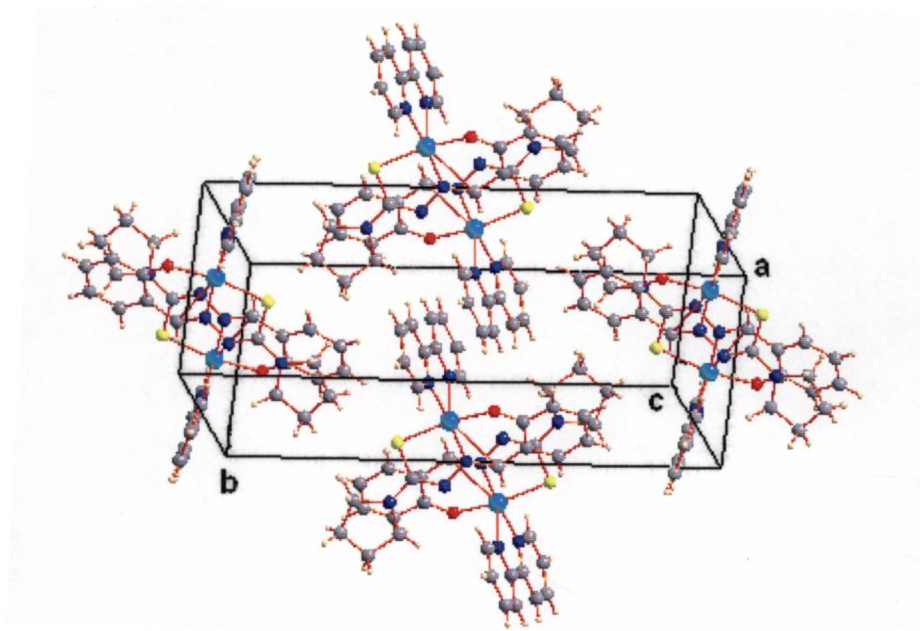


Figure 3.2. Unit cell packing diagram of the compound 10

3.3.2. IR spectra

The significant IR bands of the complexes 1–10 with their tentative assignments are presented in Table 3.5.

The IR spectra of the ligands H_2L^2 and H_2L^4 showed an intermolecular hydrogen bonded $\nu(OH)$ vibrations at 3315 and 3232 cm^{-1} respectively, which disappeared in the spectra of complexes except in 1 and 7. It is further corroborated with the downward shift of 60–80 cm^{-1} for $\nu(CO)$ as well as an appearance of a band at 390–430 cm^{-1} region due to a $\nu(Cu-O)$ stretch in the spectra of complexes [18, 19, 20]. It indicates coordination *via* phenolic oxygen.

Azomethine nitrogen bands ~ 1600 cm^{-1} in the uncomplexed thiosemicarbazones undergo a shift towards the lower energy side by 10–40 cm^{-1} in the spectra of complexes [13] due to the conjugation of the p-orbital on the double

bond with the d-orbital on the metal ion with the reduction of force constant, but with loss of proton from N, another strong band is found in the region of 1530–1555 cm^{-1} which may be due to the newly formed $\nu(\text{C}=\text{N})$ bond, resulting from enolization of the principal thiosemicarbazone ligands in the spectra for these complexes except **3** and **8**. Coordination of azomethine nitrogen is consistent with the presence of a band in the 430–480 cm^{-1} region, assignable to $\nu(\text{Cu}-\text{N})$ for these complexes [21, 22]. The increase in $\nu(\text{NN})$ in the spectra of complexes is due to enhanced double bond character through chelation, thus offsetting the loss of electron density *via* donation to the metal ion, and is supportive of azomethine coordination.

The spectral band $\nu(\text{NH})$ of thiosemicarbazones disappeared in the complexes except in **3** and **8**, indicating the deprotonation of the $-\text{NH}$ proton and coordination *via* thiolate sulfur is indicated by a decrease in stretching and bending frequencies (30–80 cm^{-1}) of the thioamide band, which is partly $\nu(\text{CS})$, and found at ~ 1320 and 840 cm^{-1} in the uncomplexed thiosemicarbazones to ~ 1270 and 750 cm^{-1} in the spectra of complexes. In complexes **3** and **8**, coordination takes place *via* thione sulfur atom. The negative shift of $\nu(\text{CS})$ in the complexes is already indicated by Campbell [2]. The $\nu(\text{CuS})$ vibration in the range 340–380 cm^{-1} further corroborates the sulfur bonding [23-25]. IR spectra of the complexes **4**, **5**, **6**, **9** and **10** exhibit bands characteristic of coordinated heterocyclic bases [26].

IR spectra of the complexes **2**, **5**, **6** and **9** are presented in Figures 3.3-3.6.

Table 3.5. Selected IR bands (cm^{-1}) with tentative assignments of the ligands and its Cu(II) complexes

Compound	$\nu(\text{OH})$	$\nu(\text{C}=\text{N}_{\text{azo}})$	$\nu(\text{C}=\text{N})$	$\nu(\text{N}-\text{N})$	$\nu/\delta[(\text{C}=\text{S})/(\text{C}-\text{S})]$	$\nu(\text{C}-\text{O})$	$\nu(\text{Cu}-\text{N})$	Bands due to heterocyclic bases
HL^1		1624	----	1066	1334, 837	----	----	----
$[\text{CuL}^1]_2 \cdot \text{H}_2\text{O}$ (1)		1587	1549	1072	1271, 753	----	463	----
H_2L^2	3315	1612	----	1037	1324, 861	1271	----	----
$[(\text{CuL}^2)_2]$ (2)		1594	1554	1083	1273, 751	1208	477	----
$[\text{Cu}(\text{HL}^2)_2]$ (3)		1585	----	1068	1310, 856	1198	453	----
$[\text{CuL}^2 \text{bipy}]$ (4)		1594	1536	1073	1271, 759	1201	461	1439, 736
$[\text{CuL}^2 \text{phen}]$ (5)		1593	1535	1082	1265, 754	1194	466	1444, 727
$[\text{CuL}^2 \gamma\text{-pic}] \cdot 2\text{H}_2\text{O}$ (6)		1596	1555	1082	1273, 751	1208	488	1437, 622
HL^3		1607	----	1064	1312, 821	----	----	----
$[\text{CuL}^3]_2 \cdot 0.5\text{H}_2\text{O}$ (7)		1595	1549	1076	1266, 730	----	453	----
H_2L^4	3442	1622	----	1034	1338, 839	1288	----	----
$[\text{Cu}(\text{HL}^4)_2]$ (8)		1605	----	1067	1325, 830	1230	437	----
$[\text{CuL}^4 \text{py}] \cdot 3\text{H}_2\text{O}$ (9)		1595	1552	1076	1260, 753	1208	486	1437, 657
$[\text{CuL}^4 \text{bipy}]$ (10)		1594	1535	1069	1276, 766	1248	440	1451, 648

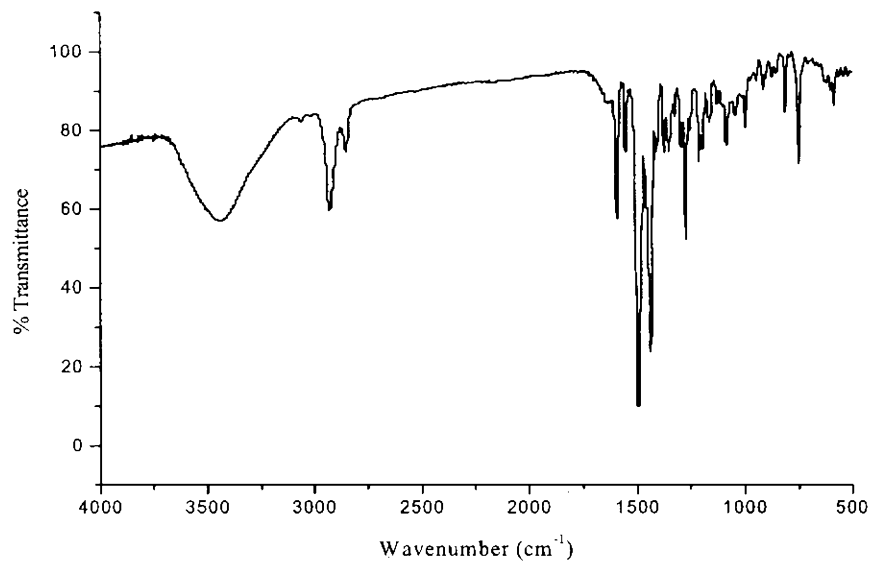


Figure 3.3. IR spectrum of the compound $[(CuL^2)_2]$ (2)

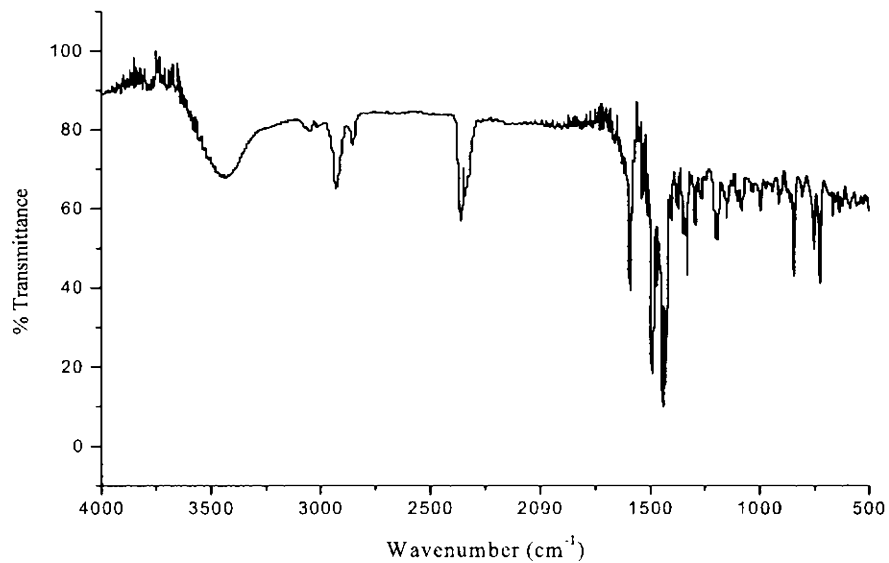


Figure 3.4. IR spectrum of the compound $[CuL^2phen]$ (5)

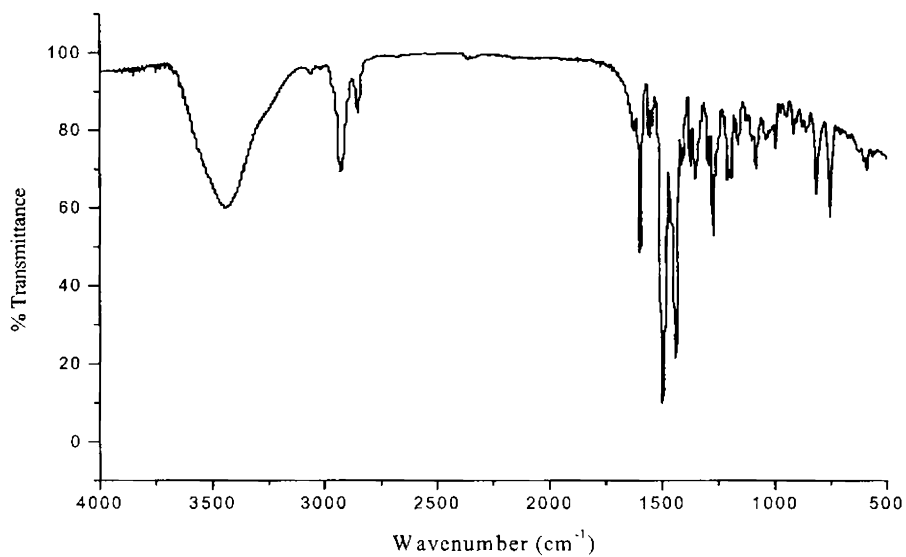


Figure 3.5. IR spectrum of the compound $[\text{CuL}^2\gamma\text{-pic}]\cdot 2\text{H}_2\text{O}$ (**6**)

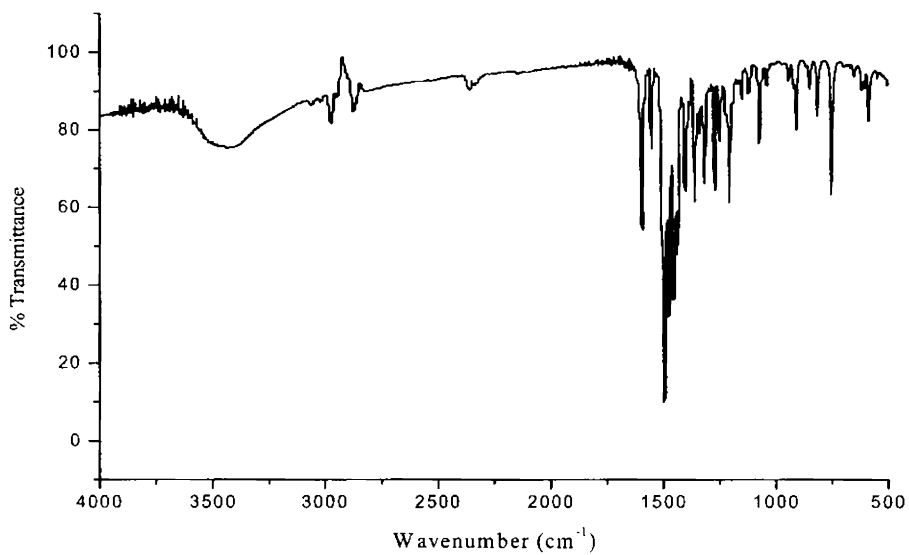


Figure 3.6. IR spectrum of the compound $[\text{CuL}^4\text{py}]\cdot 3\text{H}_2\text{O}$ (**9**)

3.3.3. Electronic spectra

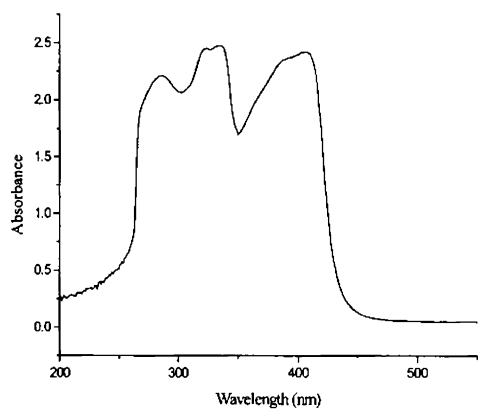
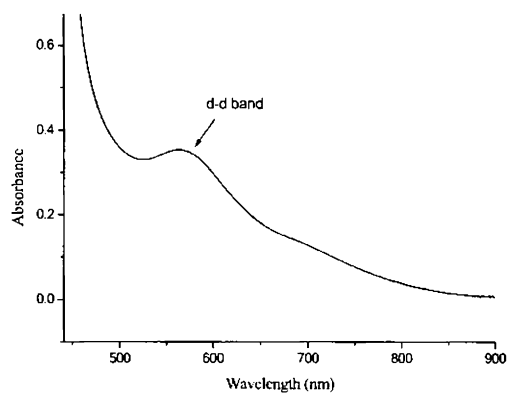
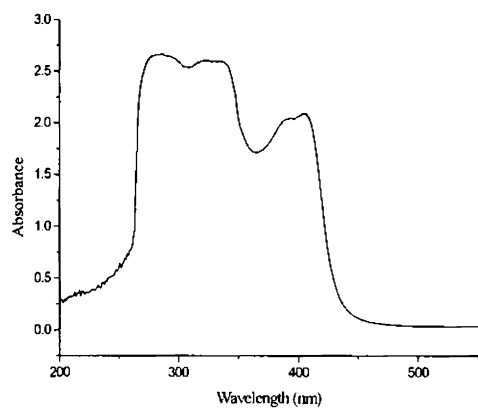
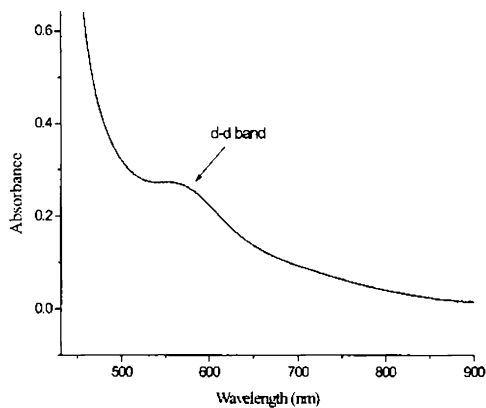
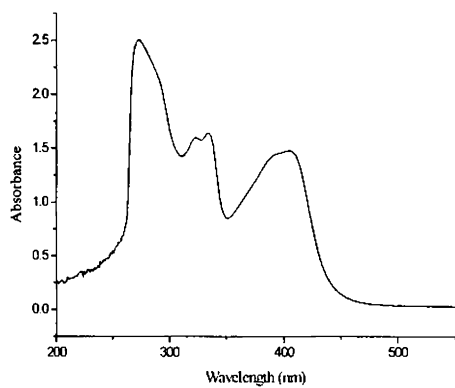
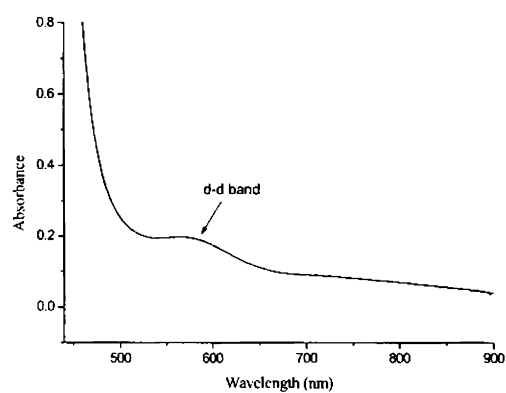
The significant electronic spectral bands for all the ligands and complexes in DMF are depicted in Table 3.6. The electronic spectra of thiosemicarbazones and its complexes show bands in the ranges 35000–37000 and 28000–32000 cm^{-1} assignable to $\pi \rightarrow \pi^*$ and $n \rightarrow \pi^*$ transitions respectively [25]. These bands are slightly shifted upon complexation. The shift of the $\pi \rightarrow \pi^*$ bands to longer wavelength region in complexes is the result of the C=S bond being weakened and the conjugation system enhanced on complexation [27, 28]. The $n \rightarrow \pi^*$ bands in the complexes have shown a blue shift due to donation of lone pair of electrons to the metal and hence the coordination of azomethine with a reduction of intensity. In the case of complexes having ONS donor ligands, the shift of two ligand to metal charge transfer bands are found in the 25000–27000 and 23000–24500 cm^{-1} ranges. In accordance with studies of previous copper(II) thiosemicarbazone complexes [29], the higher energy band is assigned to S→Cu(II) transitions. Complexes having NS donor ligands show only S→Cu(II) transitions. Its position is dependent on the steric requirements of the N(4) substituents. That is, thiosemicarbazones with bulkier N(4)-substituents have this band at somewhat higher energies. In most of the dianionic complexes, LMCT maxima of the phenolato complexes show line broadening with a tail running into the visible part of the spectrum. This may result from a phenolate to M(II) LMCT band being superimposed on the low energy side of S→M(II) LMCT. The band in the 21000–23000 cm^{-1} range involves bridging phenoxy O→Cu(II) transitions [30]. Each complex has a broad *d-d* combination band in the range 15000–17000 cm^{-1} and appears as a shoulder on the intraligand and charge transfer bands. For a square planar complex with $d_{x^2-y^2}$ ground state, three transitions are possible *viz*,

$$d_{x^2-y^2} \rightarrow d_{xy}, d_{z^2} \text{ and } d_{x^2-y^2} \rightarrow d_{xz}, d_{yz} \quad ({}^2A_{1g} \leftarrow {}^2B_{1g}, {}^2B_{2g} \leftarrow {}^2B_{1g} \text{ and } {}^2E_g \leftarrow {}^2B_{1g})$$

and square pyramidal complexes have the $d_{x^2-y^2} \rightarrow d_{xz}, d_{yz}$ and $d_{x^2-y^2} \rightarrow d_{z^2}$ transitions [31, 32]. Representative spectra of the complexes **2**, **3** and **5** are presented in Figure 3.7.

Table 3.6. Electronic spectral assignments (cm^{-1}) of the ligands and its Cu(II) complexes

Compound	$\pi - \pi^*$	$n - \pi^*$	LMCT	d - d
HL ¹	36900	28250	----	----
[CuL ¹] ₂ ·H ₂ O (1)	36360	30490	26170	15180
H ₂ L ²	36110	29500	----	----
[(CuL ²) ₂] (2)	35210	29670,31450	22330,25910	15820
[Cu(HL ²) ₂] (3)	35970	29670,31850	24330,25970	15630
[CuL ² bipy] (4)	35090	29850,31250	24330,25640	17420
[CuL ² phen] (5)	35120	29670,31200	24330,25770	17120
[CuL ² γ -pic]·2H ₂ O (6)	35210	29790,31250	24270,25990	17300
HL ³	35340	31150	----	----
[CuL ³] ₂ ·0.5H ₂ O (7)	35250	31210	25900	16640
H ₂ L ⁴	36490	30210	-----	-----
[Cu(HL ⁴) ₂] (8)	36100	31460	25380	14160
[CuL ⁴ py]·3H ₂ O (9)	35590	31450	25320	17510
[CuL ⁴ bipy] (10)	35560	31640	25250	17180

 $[(\text{CuL}^2)_2] (2)$  $[(\text{CuL}^2)_2] (2)$  $[\text{Cu}(\text{HL}^2)_2] (3)$  $[\text{Cu}(\text{HL}^2)_2] (3)$  $[\text{CuL}^2 \text{ phen}] (5)$  $[\text{CuL}^2 \text{ phen}] (5)$ **Figure 3.7.** Electronic spectra of the compounds **2**, **3** and **5** in DMF solutions

3.3.4. EPR spectra

EPR spectra of the complexes in the polycrystalline state at 298 K and in DMF at 77 K were recorded in the X-band and the g factors were quoted relative to the standard marker TCNE ($g=2.00277$). The EPR parameters of Cu(II) complexes obtained for the polycrystalline state at 298 K and in DMF at 77 K are presented in Tables 3.7 and 3.8.

EPR spectra of the complexes recorded in polycrystalline state at room temperature also provide information about the coordination environment around Cu(II) in these complexes. EPR studies of Cu(II) complexes of some salicylaldehyde thiosemicarbazones were reported earlier [25, 33]. The EPR spectra of compounds **2**, **3**, **6**, **9** and **10** in the polycrystalline state (298 K) show only one broad signal, which is attributable to enhanced spin lattice relaxation due to dipolar interaction. These type of spectra do not give any information on the electronic ground state of Cu(II) ion present in the complexes. The spectrum of compound **4** gave three g values viz. g_1 , g_2 and g_3 , which indicate rhombic distortion in their geometry. The values g_1 and g_2 are very close to each other in the compounds, which mean that rhombic distortion is very small. The lowest g value (g_1) is >2.04 indicating a rhombic, distorted square based pyramidal geometry. The spectra of compounds **1**, **5**, **7** and **8** show typical axial spectra with well-defined g_{\parallel} and g_{\perp} values. The geometric parameter G , which is a measure of the exchange interaction between the copper centers in the polycrystalline compound is calculated using the equation, $G = g_{\parallel} - 2.0023 / g_{\perp} - 2.0023$ for axial spectra and for rhombic spectra $G = g_3 - 2.0023 / g_{\perp} - 2.0023$, where $g_{\perp} = (g_1 + g_2) / 2$. If $G > 4.4$, exchange interaction is negligible and if it is less than 4.4, considerable exchange interaction is indicated in the solid complex [33, 34]. In all the Cu(II) complexes $g_{\parallel} > g_{\perp} > 2.0023$ and G value within the range 2.5–3.5 are consistent with a

$d_{x^2-y^2}$ ground state [35, 36]. The parameter R $\{R = (g_2-g_1)/(g_3-g_2)$ for rhombic systems} calculated for the compound **4** is around 0.326, *i.e.*, $R < 1$, indicating a $d_{x^2-y^2}$ ground state of the copper(II) ion [37, 38].

Table 3.7. EPR spectral assignments for Cu(II) complexes in polycrystalline state at 298 K and in DMF at 77 K

Compound	Polycrystalline state (298 K)	DMF solution (77 K)					
		g_{\parallel}	g_{\perp}	g_{av}	A_{\parallel}^a	A_{\perp}^a	A_{av}^a
[CuL ₂] \cdot H ₂ O (1)	2.141/2.050 (g_{\parallel}/g_{\perp})	2.113	2.040	2.064	164.4	25.4	70.7
[(CuL ₂) ₂] (2)	2.040 (g_{iso})	2.162	2.045	2.084	191.8	22.2	76.9
[Cu(HL ²) ₂] (3)	2.053 (g_{iso})	2.134	2.037	2.069	179.3	22.2	72.9
[CuL ² bipy] (4)	2.177/2.079/2.047 ($g_3/g_2/g_1$)	2.168	2.045	2.086	190.6	14.2	70.9
[CuL ² phen] (5)	2.192/2.059 (g_{\parallel}/g_{\perp})	2.184	2.059	2.101	----	----	----
[CuL ² γ -pic] \cdot 2H ₂ O (6)	2.067 (g_{iso})	2.169	2.047	2.088	202.5	22.3	80.1
[CuL ³ ₂] \cdot 0.5H ₂ O (7)	2.199/2.061 (g_{\parallel}/g_{\perp})	2.194	2.055	2.107	196.2	15.9	73.7
[Cu(HL ⁴) ₂] (8)	2.141/2.053 (g_{\parallel}/g_{\perp})	2.117	2.047	2.070	174.6	----	----
[CuL ⁴ py] \cdot 3H ₂ O (9)	2.047 (g_{iso})	2.155	2.042	2.080	194.5	27.0	80.9
[CuL ⁴ bipy] (10)	2.053 (g_{iso})	2.170	2.052	2.091	189.1	20.7	74.8

^a Expressed in units of cm^{-1} multiplied by a factor of 10^{-4} .

The spectra of all the complexes in DMF at 77 K are axial. The solution spectra of complexes except **5**, at 77 K in DMF show four hyperfine lines characteristic of monomeric Cu(II) complexes corresponding to $-3/2, -1/2, 1/2$ and $3/2$ transitions, which arise from the coupling of the odd electron with Cu nuclei (^{65}Cu , $I=3/2$) and spectrum of compound **5** is axial without any super or hyperfine lines. The third copper hyperfine line is expected to overlap with the high field component (g_{\perp}) in **1** and **8**. However, the half field signal corresponding to the dimer was not observed for the compound **2** [39]. The spectra of compounds **1**, **3** and **7** gave five superhyperfine lines, which arise from the coupling of the electron spin with the nuclear spin of the two nitrogen atoms in the g_{\parallel} features indicating the

coordination of two coplanar nitrogen atoms *i.e.* in each complex two azomethine nitrogens coordinate to the metal centre. The spectrum of complex **2** gave three superhyperfine lines, indicating that only azomethine nitrogen is involved in bonding in the monomer unit. This confirms the binuclear nature of the complex. In the spectra of compounds **6** and **9**, all the signals show five superhyperfine lines in the low field and five splittings in the high field region. This splitting may be due to the presence of heterocyclic bases present in the molecule *i.e.* two nitrogens involved are coplanar. The g_{\parallel} values in all these complexes are less than 2.3 is an indication of significant covalent bonding in these complexes [40, 41]. The $g_{\parallel} > g_{\perp}$ values accounts to the distorted square based pyramid structure in five coordinated complexes and rules out the possibility of a trigonal bipyramidal structure, which would be expected to have $g_{\parallel} < g_{\perp}$. For complexes **4** and **10** having bipyridine as coligand, g_{\parallel} value of **4** is smaller compared to **10** indicating that H_2L^2 is stronger ligand than H_2L^4 .

Table 3.8. EPR bonding parameters for compounds 1-10

Compound	G	R	DMF solution (77 K)							
	(298 K)		α^2	β^2	γ^2	K	K_{\parallel}	K_{\perp}	f^a	P
[CuL ¹ ₂]-H ₂ O (1)	2.94	----	0.62	0.81	0.94	0.32	0.50	0.58	128	0.0183
[(CuL ²) ₂] (2)	----	----	0.76	0.81	0.83	0.37	0.62	0.63	112.7	0.0239
[Cu(HL ²) ₂] (3)	----	----	0.68	0.81	0.83	0.33	0.55	0.57	119	0.0213
[CuL ² bipy] (4)	2.89	0.326	0.75	0.88	0.89	0.32	0.66	0.67	113.7	0.0253
[CuL ² phen] (5)	3.31	----	----	----	----	----	----	----	----	----
[CuL ² γ -pic]-2H ₂ O (6)	----	----	0.79	0.83	0.86	0.36	0.66	0.68	107	0.0256
[CuL ³]-0.5H ₂ O (7)	----	----	0.69	0.83	0.86	0.30	0.57	0.59	116.8	0.0214
[Cu(HL ⁴) ₂] (8)	2.50	----	0.66	0.77	0.95	----	0.51	0.63	121.3	----
[CuL ⁴ py]-3H ₂ O (9)	----	----	0.75	0.85	0.86	0.35	0.63	0.64	110.8	0.0236
[CuL ⁴ bipy] (10)	----	----	0.75	0.88	0.95	0.34	0.66	0.72	114.8	0.0239

^a Expressed in units of cm.

The EPR parameters g_{\parallel} , g_{\perp} , g_{av} , $A_{\parallel}(\text{Cu})$, $A_{\perp}(\text{Cu})$ and energies of $d-d$ transitions were used to evaluate the bonding parameters α^2 , β^2 and γ^2 , which may be regarded as measures of covalency of the in-plane σ -bonds, in-plane π -bonds and out-of-plane π -bonds respectively [40].

The value of in-plane σ -bonding parameter α^2 was estimated from the expression,

$$\alpha^2 = -A_{\parallel}/0.036 + (g_{\parallel} - 2.00277) + 3/7 (g_{\perp} - 2.00277) + 0.04$$

The orbital reduction factors, $K_{\parallel}^2 = \alpha^2\beta^2$ and $K_{\perp}^2 = \alpha^2\gamma^2$ were calculated using the following expressions [40, 42],

$$K_{\parallel}^2 = (g_{\parallel} - 2.00277) E_{d-d}/8\lambda_0$$

$$K_{\perp}^2 = (g_{\perp} - 2.00277) E_{d-d}/2\lambda_0$$

Where λ_0 is the spin orbit coupling constant with a value of -828 cm^{-1} for Cu(II) d^9 system.

According to Hathaway [43], for pure σ -bonding $K_{\parallel} \approx K_{\perp} \approx 0.77$, and for in-plane π -bonding, $K_{\parallel} < K_{\perp}$; while for out-of-plane π -bonding $K_{\perp} < K_{\parallel}$. In all the complexes it is observed that $K_{\parallel} < K_{\perp}$, which indicates the presence of significant in-plane π -bonding. The values of the bonding parameters α^2 , β^2 and $\gamma^2 < 1.0$ (value of 1.0 for 100% ionic character) indicate significant in-plane π -bonding and in-plane σ -bonding.

The Fermi contact hyperfine interaction term K , which is a dimensionless quantity and is generally found to have a value of 0.36, which is a measure of the contribution of 's' electrons to the hyperfine interaction can be calculated from the expression [43],

$$K = A_{iso}/P\beta^2 + (g_{av} - 2.00277) / \beta^2$$

Where P is the free ion dipolar term and its value is 0.036. The K values obtained for all the complexes are in good agreement with those estimated by Assour [44] and Abragam and Pryce [45]. The empirical factor $f = g_{\parallel} / A_{\parallel} (\text{cm}^{-1})$ is an index of tetragonal distortion. The value may vary from 105–135 for small to extreme distortion and that depends on the nature of the coordinated atom. In all the compounds except **1** and **8**, f falls in the range 105–135 corresponding to a copper(II) center with medium distortion [12]. High distortion occurs for the complexes **1** and **8** which are evidenced from the f value. Representative EPR spectra of the compounds **3**, **4** and **5** in polycrystalline state at 298 K (Figures 3.8–3.10) and **2**, **3**, **6** and **9** in DMF at 77 K are presented in Figures 3.11–3.14.

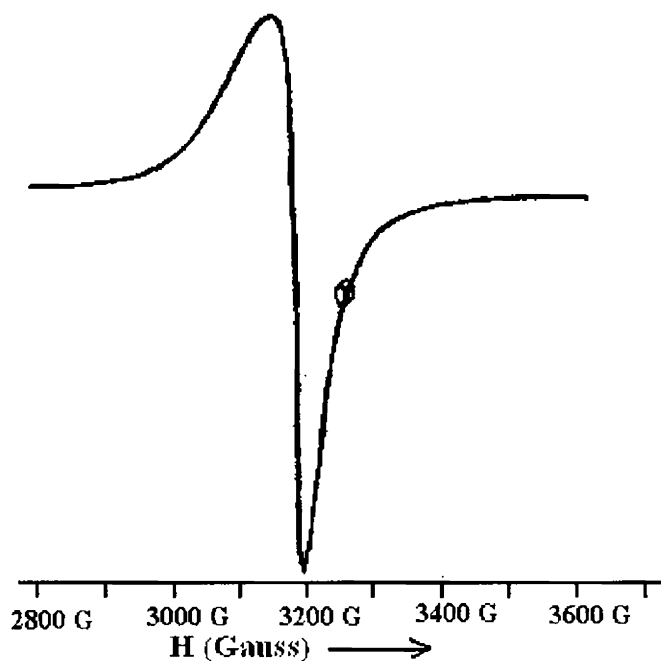


Figure 3.8. EPR spectrum of the compound $[\text{Cu}(\text{HL}^2)_2]$ (**3**) in polycrystalline state at 298 K

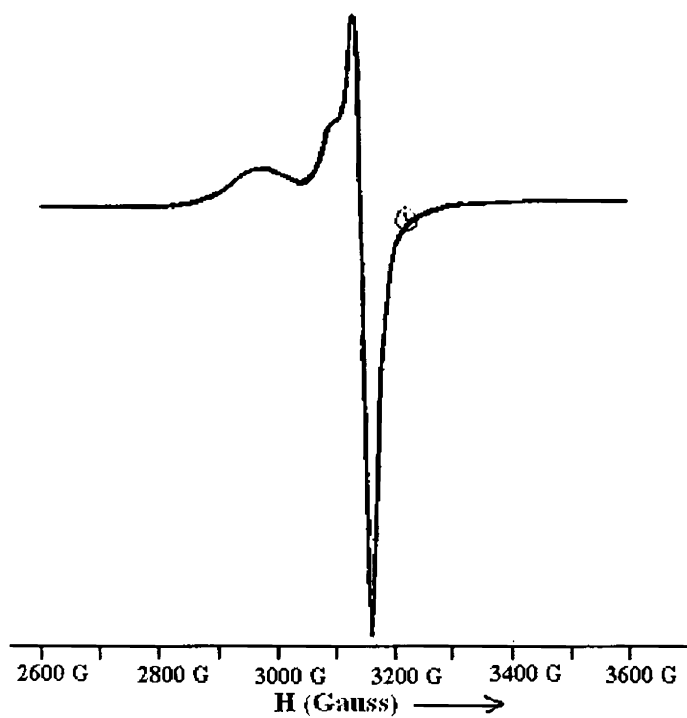


Figure 3.9. EPR spectrum of the compound $[\text{CuL}^2\text{bipy}]$ (4) in polycrystalline state at 298 K

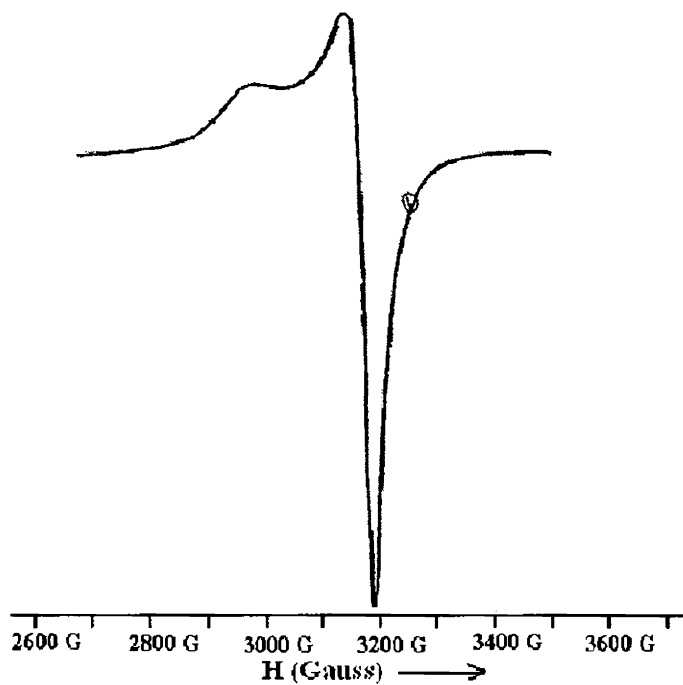


Figure 3.10. EPR spectrum of the compound $[\text{CuL}^2\text{phen}]$ (5) in polycrystalline state at 298 K

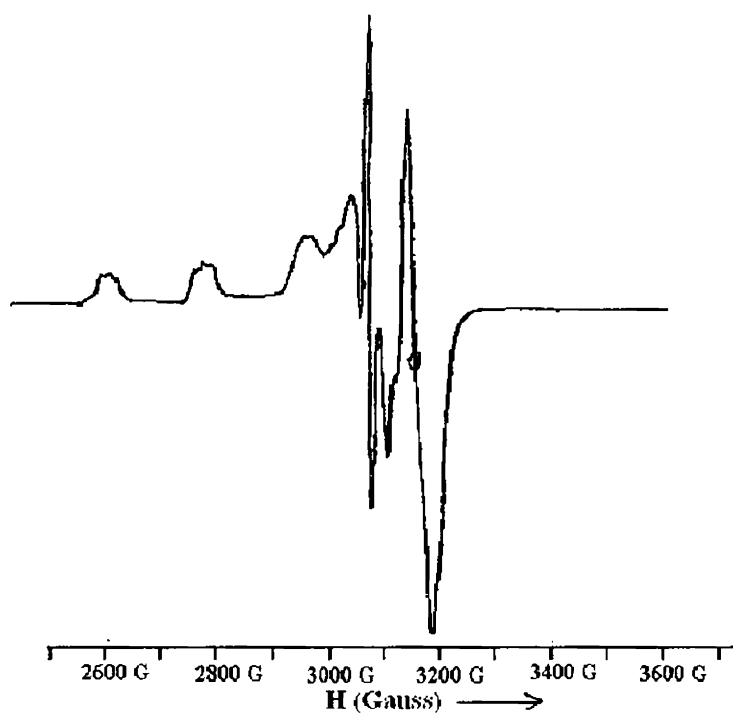


Figure 3.11. EPR spectrum of the compound $[(\text{CuL}^2)_2]$ (2) in DMF at 77 K.

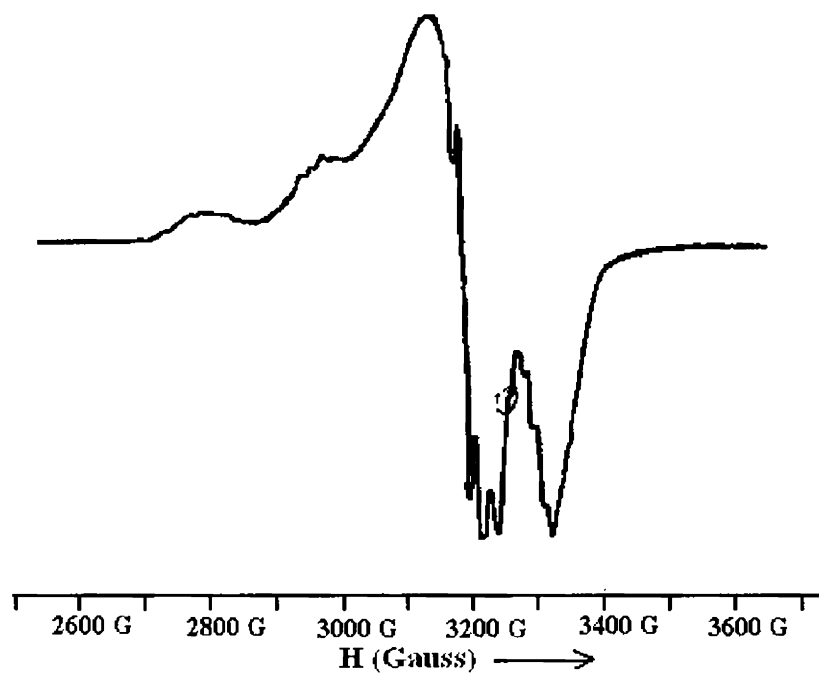


Figure 3.12. EPR spectrum of the compound $[\text{Cu}(\text{HL}^2)_2]$ (3) in DMF at 77 K.

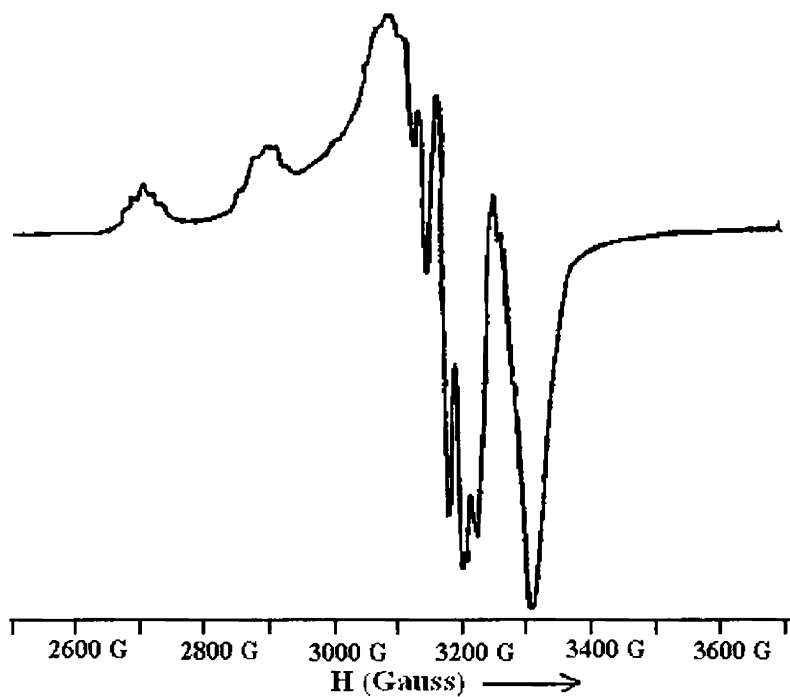


Figure 3.13. EPR spectrum of the compound $[\text{CuL}^2\gamma\text{-pic}]\cdot 2\text{H}_2\text{O}$ (6) in DMF at 77 K

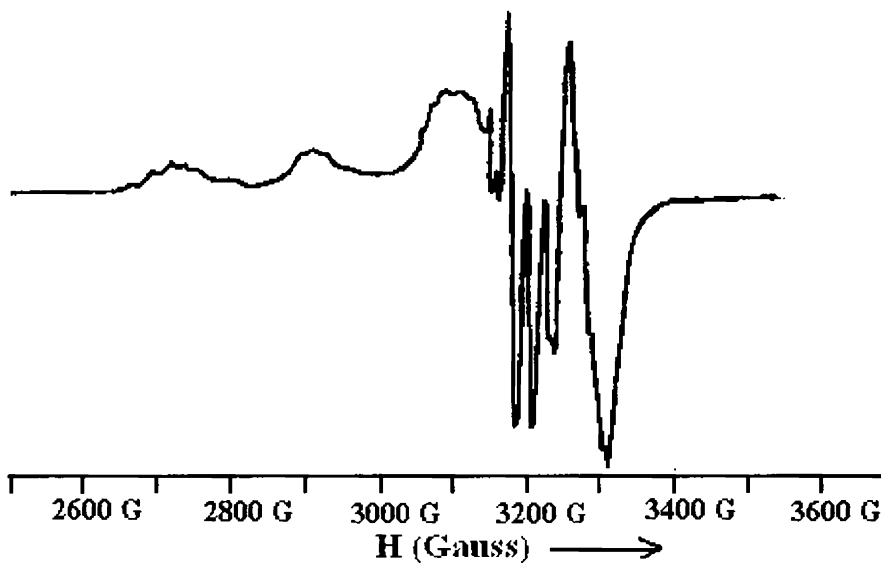


Figure 3.14. EPR spectrum of the compound $[\text{CuL}^4\text{py}]\cdot 3\text{H}_2\text{O}$ (9) in DMF at 77 K

Based on the elemental analyses and spectral investigations, following tentative structures were assigned for the complexes for which, single crystals suitable for crystallographic studies could not be isolated (Figure 3.15).

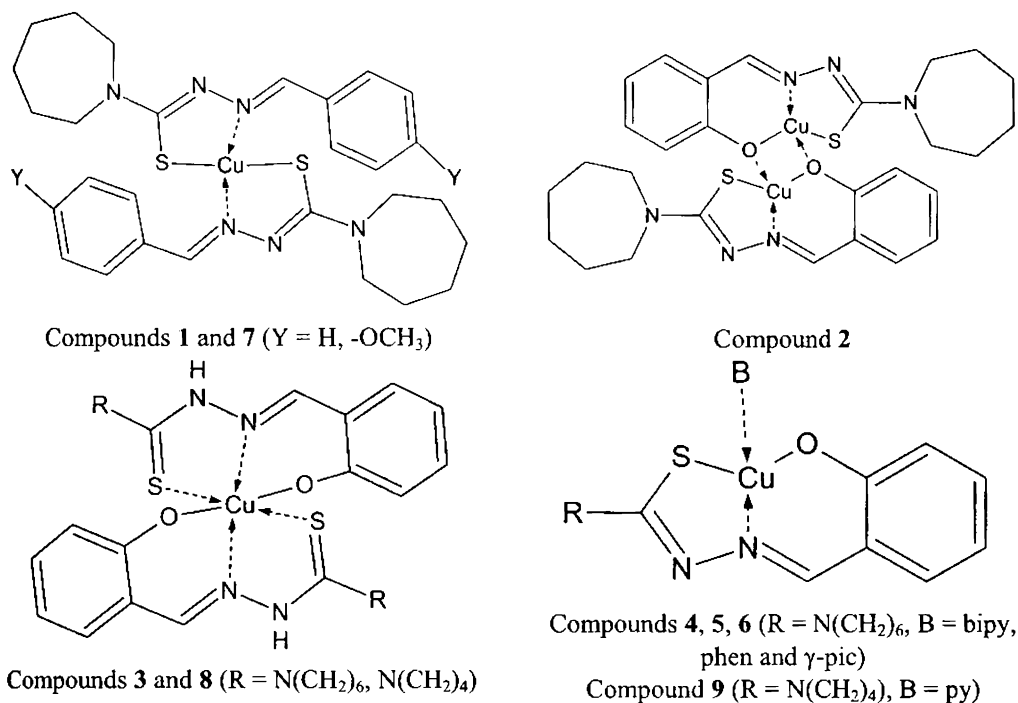


Figure 3.15. Tentative structures of the compounds

References

1. E.S. Raper, *Coord. Chem. Rev.* 153 (1996) 199.
2. M.J.M. Campbell, *Coord. Chem. Rev.* 15 (1975) 279.
3. S.B. Padhye, G.B. Kauffman, *Coord. Chem. Rev.* 63 (1985) 127.
4. D.X. West, A.E. Liberta, S.B. Padhye, R.C. Chikate, P.B. Sonawane, A.S. Kumbhar, R.G. Yerande, *Coord. Chem. Rev.* 123 (1993) 49.
5. M.B. Ferrari, S. Capacchi, G. Pelosi, G. Reffo, P. Tarasconi, R. Albertini, S. Pinelli, P. Lunghi, *Inorg. Chim. Acta* 286 (1999) 134.
6. M. A. Ali, D.A. Chowdhury, M. Nazimuddin, *Polyhedron* 3 (1984) 595.

7. Nonius (1997) MACH3 software, B.V. Nonius, Delft, The Netherlands.
8. G.M. Sheldrick, *Acta Crystallogr.* A46 (1990) 467.
9. G.M. Sheldrick, SHELXL-97 and SHELXS-97 Program for the solution of Crystal Structures, University of Göttingen, Germany, 1997.
10. K. Brandenburg, DIAMOND version 3.1d, Crystal Impact GbR, Bonn, Germany, 2006.
11. G. Plesch, C. Friebel, *Polyhedron* 14 (1995) 1185.
12. R.P. John, A. Sreekanth, V. Rajakannan, T.A. Ajith, M.R.P. Kurup, *Polyhedron* 23 (2004) 2549.
13. E.B. Seena, M.R.P. Kurup, *Polyhedron* 26 (2007) 829.
14. C.B. Castellani, G. Gatti, R. Millini, *Inorg.Chem.* 23 (1983) 4004.
15. N.J. Ray, B.J.Hathaway, *Acta Crystallogr.* B34 (1978) 3224.
16. G. Druhan, B.J.Hathaway, *Acta Crystallogr.* B35 (1979) 344.
17. A.W. Addison, T.N. Rao, J. Reedijk, J. Van Rijn, G.C. Verschoor, *J.Chem.Soc., Dalton Trans.* (1984) 1349.
18. R.C. Chikate, A.R. Belapure, S.B. Padhye, D.X. West, *Polyhedron* 24 (2005) 889.
19. V.D. Khanolkar, D.D. Khanolkar, *Indian J. Chem.* 18A (1979) 315.
20. J. Jezierska, B. Jezowska-Trzebiatowska, G. Petrova, *Inorg. Chim. Acta* 50 (1981) 153.
21. Z. Afrasiabi, E. Sinn, J. Chen, Y. Ma, A.L. Rheingold, L.N. Zakharov, N. Rath, S. Padhye, *Inorg. Chim. Acta* 357 (2004) 271.
22. R.P. John, A. Sreekanth, M.R.P. Kurup, A. Usman, I.A. Razak, H.-K. Fun, *Spectrochim. Acta* 59A (2003) 1349.
23. S.K. Sengupta, S.K. Sahni, R.N. Kapoor, *Acta. Chim. Acad. Sci. Hungary* 104 (1980) 89.

24. M. Joseph, M. Kuriakose, M.R.P. Kurup, E. Suresh, A. Kishore, S.G. Bhat, *Polyhedron* 25 (2006) 61.
25. P. Bindu, M.R.P. Kurup, T.R. Satyakeerty, *Polyhedron* 18 (1998) 321.
26. P.B. Sreeja, M.R.P. Kurup, *Spectrochim. Acta* 61A (2005) 331.
27. V. Philip, V. Suni, M.R.P. Kurup, *Polyhedron* 25 (2006) 1931.
28. I.-X. Li, H.A. Tang, Yi-Zhi Li, M. Wang, L.-F. Wang, C.-G. Xia, *J. Inorg. Biochem.* 78 (2000) 167.
29. M. Mikuriya, H. Okawa, S. Kida, *Inorg. Chim. Acta* 34 (1979) 13.
30. M. Mikuriya, H. Okawa, S. Kida, *Bull. Chem. Soc. Japan* 53 (1980) 3717.
31. P. Bindu, M.R.P. Kurup, *Trans. Met. Chem.* 22 (1997) 578.
32. I.M. Proctor, B.J. Hathaway, P. Nicholis, *J. Chem. Soc.* (1968) 1678.
33. B.J. Hathaway, D.E. Billing, *Coord. Chem. Rev.* 5 (1970) 1949.
34. A. Sreekanth, M.R.P. Kurup, *Polyhedron* 22 (2003) 3321.
35. M.J. Bew, B.J. Hathaway, R.R. Faraday, *J.Chem.Soc., Dalton Trans.* (1972) 1229.
36. S.S. Kandil, A. El-Dissouky, G.Y. Ali, *J. Coord. Chem.* 57 (2004) 105.
37. M.F. El-Shazly, A. El-Dissouky, T.M. Salem, M.M. Osman, *Inorg. Chim. Acta* 40 (1980) 1.
38. A.H. Maki, B.R. McGarvey, *J. Chem. Phys.* 29 (1958) 35.
39. P.F. Raphel, E. Manoj, M.R.P. Kurup, *Polyhedron* 26 (2007) 818.
40. J.R. Wasson, C. Trapp, *J. Phys. Chem.* 73 (1969) 3763.
41. D. Kivelson, R. Neiman, *J.Chem.Soc., Dalton Trans.* 35 (1961) 149.
42. B.J. Hathaway, *Structure and Bonding*, Springer Verlag, Heidelberg, (1973) 60.
43. R.S. Nicholson, *Anal. Chem.* 37 (1965) 1351.
44. M. Assour, *J. Chem. Phys.* 43 (1965) 2477.
45. A. Abragam, M.H.L. Pryce, *Proc. R. Soc. London A206* (1961) 164.